Proceedings of the 2nd Biennial IEEE/RAS-EMBS International Conference on Biomedical Robotics and Biomechatronics
Scottsdale, AZ, USA, October 19-22, 2008

Dynamics of Escaping Flight Initiations of *Drosophila melanogaster*

Francisco A. Zabala[§], Gwyneth M. Card, Ebraheem I. Fontaine,
Richard M. Murray, and Michael H. Dickinson
Division of Engineering and Applied Science
California Institute of Technology
Pasadena, California 91125
[§]Author for correspondence (e-mail: fzabala@cds.caltech.edu)

***Abstract*— We present a reconstruction of the dynamics of flight initiation from kinematic data extracted from high-speed video recordings of the fruit fly *Drosophila melanogaster*. The dichotomy observed in this insect's flight initiation sequences, generated by the presence or absence of visual stimuli, clearly generates two contrasting sets of dynamics once the flies become airborne. By calculating reaction forces and moments using the unconstrained motion formulation for a rigid body, we assess the fly's responses amidst these two dynamic patterns as a step towards refining our understanding of insect flight control.**

I. Introduction

Difficulties inherent to the miniaturization of unmanned aircraft have evoked studies of biological mechanisms for the development of innovative means of perception, actuation, and control. Particular interest has been put into characterizing insect flight, where these three components seem to interact quite effectively. This reverse engineering feat has not been without challenges; roughly, we can classify these challenges into three major categories: 1) modeling sensors (particularly vision), [1]–[3], and actuators (unsteady effects of flapping), [4]–[6]; 2) mapping variations of wing and body kinematics to the production of aerodynamic forces and moments, [7]–[11]; and 3) understanding mechano-sensorial connections that trigger such kinematic variations, [12]–[20]. Further difficulties are also faced at a higher stratus of insect flight control, in particular, recognizing patterns of behavior and understanding decision-making processes [21]. Figure 1 illustrates the authors' view of the macroscopic components of insect flight control, and the general approaches followed for its study, as presented in literature [1]–[20].

While simplified aerodynamic models give us acceptable estimates of the insect's production of forces and moments, other simplifications and assumptions limit a comprehensive understanding of insect flight

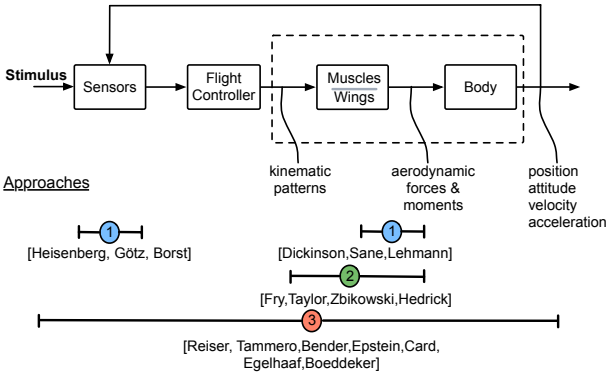

Fig. 1. Macroscopic Components of Insect Flight Control. ①, ②, and ③ represent the areas where the study of flight control has focused. Last names correspond to most representative references included in this text.

control. In the past, empirical assessments of the relation between wing and body kinematics, and the production of aerodynamic forces and moments have been made by studying two flight conditions, namely, hovering and stable forward flight. Under these conditions, plausible responses to small perturbations about the insect's desired operating point have been investigated [9]–[11]. Naturally, this leads to two important questions: What occurs when the perturbations are not small? Does the insect consistently produce the same forces and moments to counteract these perturbations? Our current framework is aimed at answering these questions, with the underlying motivation of refining our current understanding of insect flight control.

A way of approaching the study of insect flight control has been by triggering consistent behaviors, and characterizing specific outcomes. In particular, this approach has yielded interesting results in the study of visually elicited saccadic turns in free-flight [15] and tethered insects [16], [19], as well as in simulation environments

978-1-4244-2883-0/08/$25.00 ©2008 IEEE

[12], [14], [17], [18], [20], [22]. Another instance of such consistent behaviors has been identified during the flight initiation of the insect *Drosophila melanogaster* [13], [23]–[26]. In this case, the presence or absence of a visual stimulus [23]–[26] yields clearly distinct flight patterns [13].

Our approach for this study consists of using extracted kinematic data (i.e., rotational and translational positions, velocities and accelerations) from high-speed video recordings of flight initiations of the fruit fly *Drosophila melanogaster* [13] to derive the flight dynamics of each insect. In particular, we use the responses in the absence of stimuli as our nominal flight initiation model, and investigate the perturbations in the dynamics introduced by the presence of such stimuli.

The paper is divided into four sections; Section II gives an overview of the flight initiation phenomenon in *Drosophila melanogaster*, and outlines the conclusions presented in the founding work that led to this study [13]. In Section III we present our reconstruction of the dynamics of flight initiation, which is followed by a discussion of the modulation of aerodynamic forces and moments during takeoff; we conclude in Section IV summarizing the work and discussing our intents for future directions.

II. Kinematic Analysis of Flight Initiation of *Drosophila*

A. Coordinate Frames, Transformations and Notation

The following figure summarizes the coordinate frames used throughout this paper:

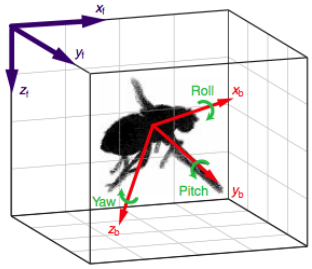

Fig. 2. The two coordinate frames used in the paper.

We employ standard aerodynamic coordinate frames to describe the motion of the insect in 3D space. We use a (lab-) earth-fixed coordinate frame (x_f, y_f, z_f) and a body-centered one (x_b, y_b, z_b)—alternatively denoted as roll, pitch, and yaw—as presented traditionally in aerodynamics literature [27].

B. Flight initiation of Drosophila melanogaster

During flight initiation, insects must transition between walking (usually at zero velocity, i.e., standing still) and flying in a way that allows them to propel off the ground without damaging their wings [23]. For the fruit fly, taking off is a process that comprises a quick extension of the legs, in tandem with the first few wing strokes. The main thrust for this study comes from the identification of two modes of flight initiation in *Drosophila* [23]–[26], one of which results in tumbling flights where the insect translates faster, but also rotates rapidly around its three body-centered axes [13]. Figures 3 and 4 illustrate this phenomenon.

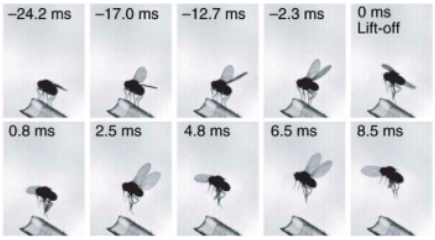

Fig. 3. Voluntary Flight Initiation. Prior wing elevation (-24.2ms – -12.7ms), and simultaneous leg-extension and wing depression (-2.3ms – 0ms) lead to a steady controlled flight initiation (0.8ms – 8.5ms).

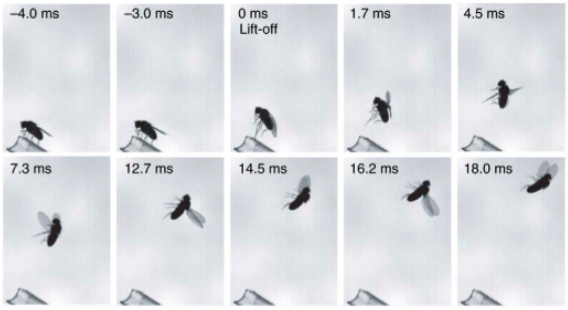

Fig. 4. Escape Flight Initiation. Leg extension begins prior to wing elevation (-3.0ms – 0ms), this leads to flight initiation without coordinated leg-extension and wing-depression (0ms), which in turn results in tumbling flight (7.3ms – 18.0ms+).

These tumbling flights, which exhibit large, transient instabilities in comparison with nominal (i.e., non-escaping) flight initiation trajectories, promote a new interpretation of the insect's flight control mechanisms beyond typical *a priori* assumptions of small deviations around an operating point. Moreover, the contrasting nature of the two modes of flight initiation motivates an explicit comparison between them using control theory criteria (e.g., stability, performance, robustness, etc.).

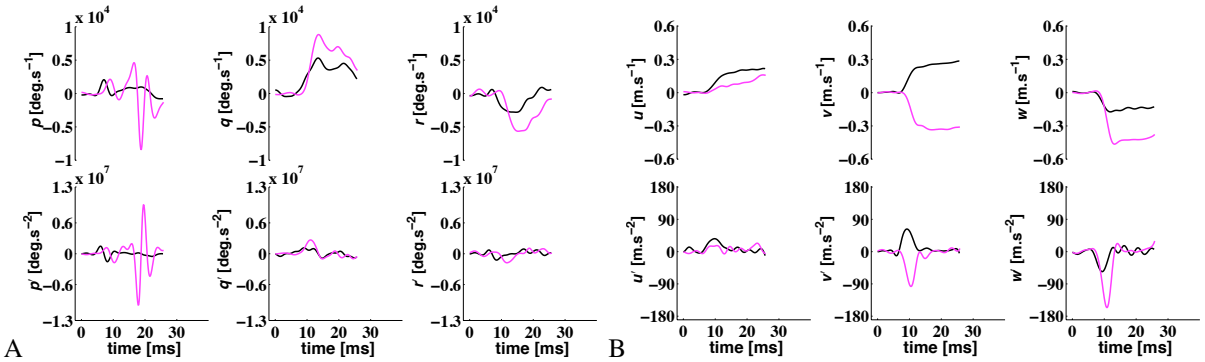

Fig. 5. Entire sequence for kinematics ([A] rotational, [B] translational) during flight initiation of a couple of fruit flies. Black (dark gray) trace shows a voluntary take-off while magenta (light gray) corresponds to an escape response. Rotational kinematics $\{(p, q, r, \dot{p}, \dot{q}, \dot{r})\}$ are measured in the body-fixed frame, while the translational are given relative to the lab-fixed frame $\{(u, v, w, \dot{u}, \dot{v}, \dot{w})\}$. Note that the symbol ($'$) in the subplots is meant to indicate ($\dot{}$).

C. Body Kinematics

In [13], the kinematics of flight initiation for a set of fruit flies were analyzed, and insightful results were obtained. We present in Figure 5 a motivating example where two (different) flies remain in the field of view of the cameras for similar periods of time, in separate ocassions. The black (darker grey) trace corresponds to a fly performing a voluntary take-off, while the magenta (lighter grey) corresponds to one executing an escape response. These data include rotational as well as translational rates $\{(p, q, r),(u, v, w)\}$ and accelerations $\{(\dot{p}, \dot{q}, \dot{r}),(\dot{u}, \dot{v}, \dot{w})\}$ relative to the body- (x_b, y_b, z_b) and lab-fixed (x_f, y_f, z_f) coordinate reference frames, respectively (e.g., $\dot{v}$ indicates the translational acceleration of the fruit fly with respect to the lab-fixed y_f axis).

We observe that besides a noticeable difference in amplitude, the two sets of responses have very similar patterns. This consistency was found in several pairs of flies (one voluntary, and one escape), and it served as additional motivation for investigating the differences and similarities under these two 'conditions' for initiating flight. Notice that in the example illustrated in Figure 5 the major difference between voluntary and escape data is observed in the rotational kinematics about the longitudinal axis of the fly $(p, \dot{p})$—this difference is representative of the entire data, see [13] for details. In Section III we analyze the dynamics of rotation in escape and voluntary flight initiations, and we rationalize this striking behavior.

Studying the dynamic responses during take-off also required us to align the kinematic data at the instant in time where each flight initiation occurred, for this purpose we utilized the acceleration spike in the vertical direction (clearly seen in the bottom-rightmost subplot of Figure 5 where the data has not been aligned yet).

III. Analysis of Flight Initiation Dynamics

In this section, we use the kinematic data described above to derive forces and moments acting on the body in order to investigate the dynamics of voluntary and escape flight initiations.

A. Mechanics of Unconstrained Motion

Applying Newton's second law, the system of equations

$$\begin{aligned} \mathbf{F}_{\mathrm{T}}(t) &= m\,\dot{\mathbf{V}}(t) + \boldsymbol{\omega}(t) \times (m\mathbf{V}(t)) \\ \mathbf{M}_{\mathrm{T}}(t) &= [\mathbf{I}]\,\dot{\boldsymbol{\omega}}(t) + \boldsymbol{\omega}(t) \times ([\mathbf{I}]\,\boldsymbol{\omega}(t)), \end{aligned} \tag{1}$$

describes the forces and moments about the 6DOF in which an object can move in 3D space [27]. Boldface notation is used to indicate vectorial quantities, and the overdot ($\dot{}$) is used to denote derivatives with respect to time. Additionally, $\mathbf{F}_{\mathrm{T}}$ denotes the total force, which lumps insect's weight, air resistance, leg forces, and wing forces; $\mathbf{M}_{\mathrm{T}}$ denotes the net moment about the origin (located at the estimated center of mass)—another lumped quantity; m denotes the mass of the fly (m = 1 [mg]); $\mathbf{V}$ and $\boldsymbol{\omega}$ denote the translational and rotational velocity vectors, respectively; and $[\mathbf{I}]$ denotes the inertia tensor.

These reaction forces and moments are illustrated in Figure 6 during voluntary (A,B,E,F) and escape (C,D,G,H) takeoffs. Traces for all flies are included, and a particular pair of them—one voluntary, and one escape—have been selected (black traces) to represent the overall dynamic behavior. For the force data (A,C), the top traces represent the x-y-z components of $\mathbf{F}^1 = m\,\dot{\mathbf{V}}$, where the superscript is used for indicating the first (or second) right-hand side term in the corresponding equation in (1). The middle traces correspond to $\mathbf{F}^2$ =

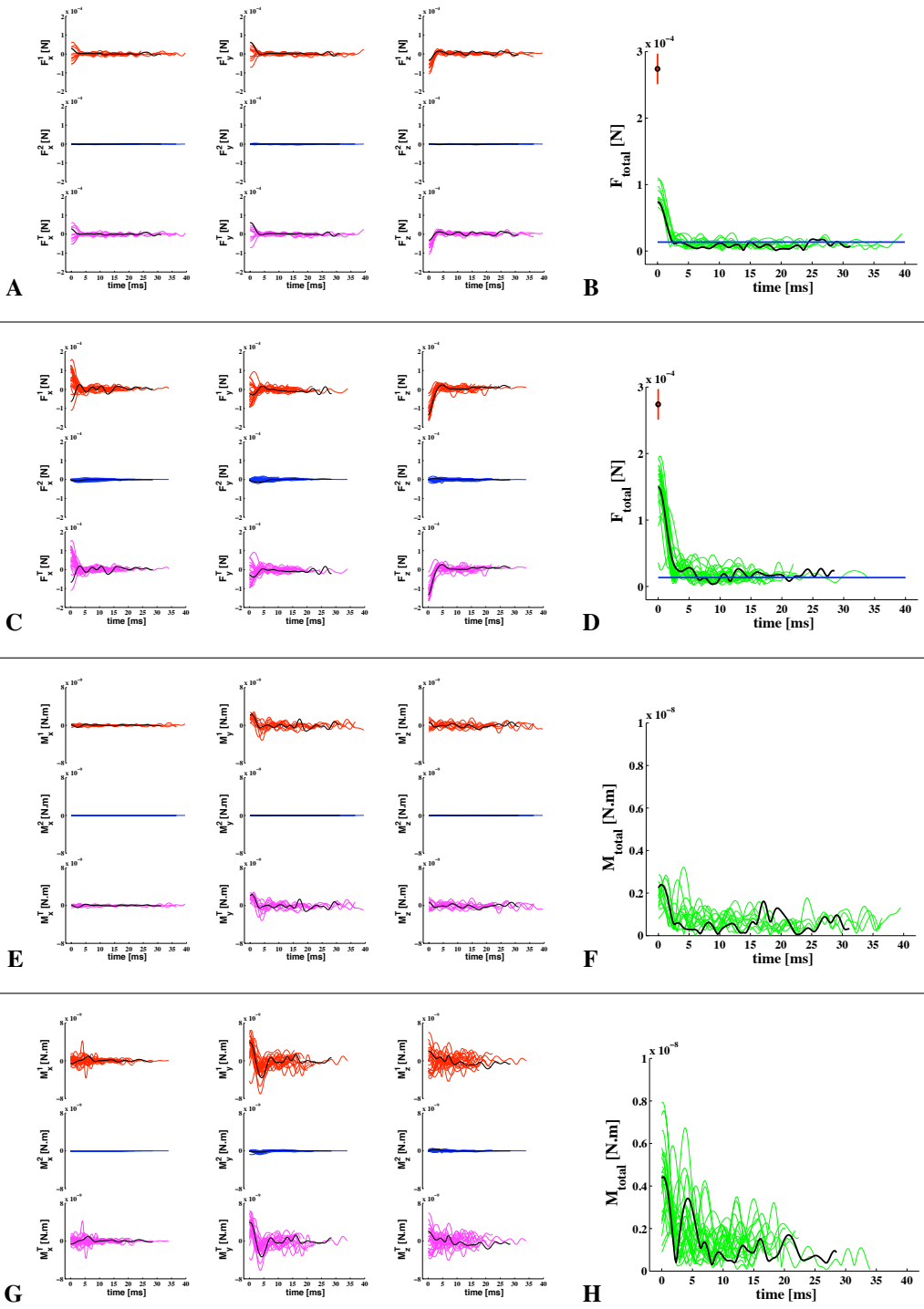

Fig. 6. Reaction forces and moments during voluntary (A,B,E,F) and escape (C,D,G,H) take-offs. The black traces correspond to individual flies (one for escape data, another for voluntary) selected to represent the overall dynamic behavior. For the force data (A and C), the top traces represent the *x*-*y*-*z* components of the first term on the right-hand side of (1), while the middle traces correspond to the second term. The bottom traces show the total force, and its magnitude is depicted in B and D. The presentation of the moment data (E,F,G,H) is analogous. The solid, horizontal trace, and the data point at 0 [ms] in B and D correspond to comparable results reported in literature: the data point (274 [μN]) corresponds to the force produced by the legs of flies in response to a visual stimulus [28] (comparable to our escape data); meanwhile, the horizontal trace (20.1 [μN]) represents the average force produced by the wings during forward flight [29] (comparable to both sets of data). Results in literature describing moment data are not suitable for comparison with ours.

$\boldsymbol{\omega}\times(m\mathbf{V})$. Finally, the bottom traces show the total force, $\mathbf{F}_{\mathrm{T}}$, while its total magnitude is depicted in the right half of the figure (B,D). The moment data (E,F,G,H) is presented in an analogous manner.

B. Discussion

We observe that the initial forces (at 0 [ms]) generated during escaping takeoffs exceed those corresponding to voluntary ones (net forces almost double). Although, given that a considerable subset of escaping takeoffs take place without wing depression (i.e., the first wingbeat occurs *after* losing contact with the substrate), and their dynamics are similar to those that do include an initial wingbeat (in terms of magnitude), we can assess that the main difference between forces generated in the two types of flight initiation relates to the jump (a more detailed justification is given in [13]). Moreover, given the kinematic behavior of escaping responses [13], we understand that 1) leg forces play a crucial role in the steadiness of flight initiations, and 2) wing forces are not sufficient to guarantee a steady takeoff in visually elicited responses.

The moments produced during flight initiations (Figure 6) are based on an approximation of the shape of the fly by a cylinder. Recall that the moment of inertia tensor for a cylinder comprises three principal components $I_{xx} = \frac{1}{2}(mR^2), I_{yy} = I_{zz} = \frac{1}{12}(mL^2) + \frac{1}{4}(mR^2)$, and six off-diagonal terms $I_{xy} = I_{yx} = I_{xz} = I_{zx} = I_{yz} = I_{zy} = 0$. Solving for M_x in (1):

$$M_x = I_{xx}\,\dot{p} + (I_{zz} - I_{yy})\,qr\,, \text{ where } (I_{zz} - I_{yy}) = 0\,, \qquad (2)$$

which implies that the insect's moment about the x_b-axis is approximately proportional to the rotational acceleration about this axis irrespective of coupling (the approximation would be exact if the fly's shape would actually be a cylinder). According to the kinematic data [13], the most significant dissimilarity between voluntary and escape flight initiations corresponds to the rotational rate and acceleration about this axis. Based on our earlier assessment about the difference in forces generated during voluntary and escape takeoffs, we center our attention at time $t = 0$ [ms]. However, we are limited in this set of experiments by the fact that forces and moments were not measured directly (as produced by the insect), and thus, we carefully interpret the results.

Typical values for longitudinal and radial lengths of *Drosophila* are $L = 2.5$ [mm], and $R = 0.7$ [mm] [7]. If we use these values to calculate our simplified moment of inertia tensor, we have

$$I_{yy} = I_{zz} = \tfrac{386}{147} I_{xx} \approx 2.6\, I_{xx}\,. \qquad (3)$$

And so, given that peak rotational rates with respect to the x_b-axis during escape responses were more than three times those observed during voluntary ones, while the peak rotational rates about the other two axes, y_b and z_b, were roughly twice as large [13]. Then, the lower moment of inertia about the x_b-axis—in comparison with the other two body axes (3)—could partially account for the difference in rotational rates about the three body axes, depending on the torques generated by the fly during takeoff.

We can also consider 'lateral' and 'longitudinal', $\mathbf{F}_{\mathrm{lat}} := \sqrt{(\mathbf{F}^{\mathrm{T}}_z)^2 + (\mathbf{F}^{\mathrm{T}}_y)^2}$, and $\mathbf{F}_{\mathrm{lon}} := \sqrt{(\mathbf{F}^{\mathrm{T}}_z)^2 + (\mathbf{F}^{\mathrm{T}}_x)^2}$, components of the initial forces; a significant difference between them (e.g., $\mathbf{F}_{\mathrm{lat}}[t = 0] >> \mathbf{F}_{\mathrm{lon}}[t = 0]$) could also account for an increase in the rotation about x- or y-axis during escaping takeoffs.

A third possibility could be an asymmetry in the forces generated by each leg, which would result if the insect actually produced different forces with its muscles, or if the legs lost contact with the ground at different times. Given that the data do not offer details about leg-specific kinematics, we are unable to assess this hypothesis concretely. We can, however, expand the left hand side of (1) by decomposing the total force as,

$$\begin{aligned} \mathbf{F}_{\mathrm{T}}(t) &= \mathbf{F}_{\mathrm{A}}(t) + \mathbf{F}_{\mathrm{L}}(t) + \mathbf{U}(t) + \mathbf{W}\,, \text{ where} \\ \mathbf{F}_{\mathrm{A}}(t) &= f(\alpha(t), \phi(t), \ldots)\,, \text{ and} \\ \mathbf{F}_{\mathrm{L}}(t) &= g(\xi(t), \psi(t), \ldots)\,. \end{aligned} \qquad (4)$$

Using $\mathbf{W}$ to denote the insect's weight vector, $\mathbf{U}(t)$ to denote air resistance, $\mathbf{F}_{\mathrm{A}}(t)$ to denote the aerodynamic force produced by the insect's wings; $f : S \to \mathbb{R}^3$ to indicate the mapping of the n-dimensional space $S = \{\alpha(t), \phi(t), \ldots\}$ (of n different wing kinematic parameters) to wing forces; $\mathbf{F}_{\mathrm{L}}(t)$ to denote the force produced by the legs; and $g : Q \to \mathbb{R}^3$ to indicate the mapping of the j-dimensional space $Q = \{\xi(t), \psi(t), \ldots\}$ (of j different leg kinematic parameters) to leg forces.

This expansion (4) allows us to establish at least two comparisons between our results and those in literature. Since leg forces are only active for as long as there is contact with the substrate, first, we consider our initial forces ($t = 0$ [ms]), which averaged to 97.3 ± 5.1 [μN] for voluntary, and 173.1 ± 20.1 [μN] for escaping takeoffs; mean±s.d.; $n = 12, 23$ respectively. And, we compare them to those reported by Zumstein *et al*, which were measured during visually elicited takeoffs and peaked at 274 [μN] [28]. These measurements were made in tethered flies and the results were highly dependent on 'leg angles', which could partially account for our underestimates. Secondly, since the unsteady dynamics induced by the jump become negligible after a certain

period of time (particular to each individual fly), the 'tail' of our dynamic data approximate the sum of aerodynamic forces produced by the insect's wings, the effect of gravity, and the air resistance. Neglecting the effects of air resistance, these estimates are similar to those in literature where it is found that the maximum average force produced throughout a wingstroke (for *Drosophila melanogaster*) is around 200% of body weight (approximately 20.1μN) [29].

IV. Conclusions and Future Work

In this paper we presented a framework for studying the dynamics of flight initiation in *Drosophila*. The reconstruction of kinematic data of the fruit fly's takeoff allowed the derivation of the forces and moments experienced by the animal. The importance of flight initiation behavior in this particular study is that it allowed, in a consistent manner, the observation of the insect's response while undergoing different dynamics. Thus, an emergent direction from this study is characterizing such response as a function of the insect's wing kinematic patterns (the wings constitute the only active actuation mechanism after take-off). Understanding how aerodynamic forces and moments are produced is essential to fully assess the dynamic behavior of the fly.

Another emergent aspect from this study is the assessment of some of the disturbances that must be handled by the insect's flight controller. We have observed throughout this paper that this is a salient feature during the escaping takeoffs, where large rotation rates need to be mitigated. Thus, a future direction that we shall follow is to study the transient 'impulsive' disturbances introduced by the fly's jump in relation to the leg kinematics; and subsequently, to assess the fly's response to them.

References

[1] M. Heisenberg and R. Wolf, *Vision in* Drosophila. Springer-Verlag New York, 1984.

[2] K. Götz, "Flight control in *Drosophila* by visual perception of motion," *Biol. Cybern.*, vol. 4, no. 6, pp. 199–208, 1968.

[3] A. Borst, "Modelling fly motion vision," *Comp. Neurosc.*, pp. 401–434, 2001.

[4] M. H. Dickinson, F.-O. Lehmann, and S. P. Sane, "Wing rotation and the aerodynamics of insect flight," *Science*, vol. 284, pp. 1954–1960, June 1999.

[5] S. Sane and M. Dickinson, "The aerodynamic effects of wing rotation and a revised quasi-steady model of flapping flight," *J. Exp. Biol.*, vol. 205, pp. 1087–1096, 2002.

[6] F. Lehmann and M. Dickinson, "The control of wing kinematics and flight forces in fruit flies (*Drosophila spp.*)," *J. Exp. Biol.*, vol. 201, pp. 385–401, 1998.

[7] S. N. Fry, R. Sayaman, and M. H. Dickinson, "The aerodynamics of free-flight maneuvers in *Drosophila*," *Science*, vol. 300, pp. 495–498, Apr. 2003.

[8] ——, "The aerodynamics of hovering flight in *Drosophila*," *J. Exp. Biol.*, vol. 208, pp. 2303–2318, 2005.

[9] G. K. Taylor and A. L. R. Thomas, "Dynamic flight stability in the desert locust *Schistocerca gregaria*," *J. Exp. Biol.*, vol. 76, pp. 449–471, 2001.

[10] R. Żbikowski, S. A. Ansari, and K. Knowles, "On mathematical modelling of insect flight dynamics in the context of micro air vehicles," *Bioinspiration and Biomimetics–learning from nature, IOP*, vol. 1, no. 2, pp. 26–37, 2006.

[11] T. Hedrick and T. Daniel, "Flight control in the hawkmoth *Manduca sexta*: the inverse problem of hovering," *J. Exp. Biol.*, vol. 209, pp. 3114–3130, 2006.

[12] M. Epstein, S. Waydo, S. B. Fuller, W. Dickson, A. Straw, M. H. Dickinson, and R. M. Murray, "Biologically inspired feedback design for *Drosophila* flight," in *Proc. IEEE American Control Conference (ACC'07)*, New York, USA, July 2007, pp. 3395–3401.

[13] G. Card and M. Dickinson, "Performance trade-offs in the flight initiation of *Drosophila*," *J. Exp. Biol.*, vol. 211, pp. 341–353, 2008.

[14] M. Egelhaaf, "Dynamic properties of two control systems underlying visually guided turning in house-flies," *J. Comp. Physiol. A*, vol. 161, no. 6, pp. 777–783, 1987.

[15] L. Tammero and M. Dickinson, "The influence of visual landscape on the free flight behavior of the fruit fly Drosophila melanogaster," *Journal of Experimental Biology*, vol. 205, pp. 327–343, 2002.

[16] L. Tammero, M. Frye, and M. Dickinson, "Spatial organization of visuomotor reflexes in Drosophila," *J. Exp. Biol.*, vol. 207, pp. 113–122, 2004.

[17] N. Boeddeker, R. Kern, and M. Egelhaaf, "Chasing a dummy target: smooth pursuit and velocity control in male blowflies." *Proc. R. Soc. B*, vol. 270, no. 1513, p. 393, 2003.

[18] N. Boeddeker and M. Egelhaaf, "Steering a virtual blowfly: simulation of visual pursuit," *Proc. Biol. Sc.*, vol. 270, no. 1527, pp. 1971–1978, 2003.

[19] J. Bender and M. Dickinson, "Visual stimulation of saccades in magnetically tethered *Drosophila*," *J. Exp. Biol.*, vol. 209, pp. 3170–3181, 2006.

[20] M. Reiser and M. Dickinson, "A test bed for insect-inspired robotic control," *Phil. Trans. Ma. Physical Eng. Sc.*, vol. 361, no. 1811, pp. 2267–2285, 2003.

[21] G. Maimon, A. Straw, and M. Dickinson, "A Simple Vision-Based Algorithm for Decision Making in Flying Drosophila," *Current Biology*, 2008.

[22] N. Boeddeker and M. Egelhaaf, "A single control system for smooth and saccade-like pursuit in blowflies," *J. Exp. Biol.*, vol. 208, pp. 1563–1572, 2005.

[23] J. R. Trimarchi and D. M. Schneiderman, "Giant fiber activation of an intrinsic muscle in the mesothoracic leg of *Drosophila melanogaster*," *J. Exp. Biol.*, vol. 177, pp. 149–167, 1993.

[24] J. Trimarchi and A. Schneiderman, "Flight initiations in *Drosophila melanogaster* are mediated by several distinct motor patterns," *J. Comp. Physiol. A: Sensory, Neural, and Behavioral Physiology*, vol. 176, no. 3, pp. 355–364, 1995.

[25] S. Hammond and M. O'Shea, "Escape flight initiation in the fly," *J. Comp. Physiol. A*, vol. 193, pp. 471–476, 2007.

[26] ——, "Ontogeny of flight initiation in the fly *Drosophila melanogaster*: implications for the giant fiber system," *J. Exp. Biol.*, vol. 211, pp. 341–353, 2008.

[27] W. F. Phillips, *Mechanics of Flight*. Hoboken, NJ: John Wiley & Sons, 2004.

[28] N. Zumstein, O. Forman, U. Nongthomba, J. C. Sparrow, and C. J. H. Elliott, "Distance and force production during jumping in wild-type and mutant *Drosophila melanogaster*," *J. Exp. Biol.*, vol. 207, pp. 3515–3522, 2004.

[29] F. Lehmann and M. Dickinson, "The changes in power requirements and muscle efficiency during elevated force production in the fruit fly *Drosophila melanogaster*," *J. Exp. Biol.*, vol. 200, no. 7, pp. 1133–1143, 1997.